

Design and motion planning of body-in-white assembly cells

Stefania Pellegrinelli^{1,2,3}, Nicola Pedrocchi¹, Lorenzo Molinari Tosatti¹, Anath Fischer², Tullio Tolio^{1,3}

Abstract—This paper proposes a method for the automatic and simultaneous identification of the body-in-white assembly cell design and motion plan. The method solution is based on an iterative algorithm that looks for a global optimum by iteratively identifying the optimum of three sub-problems. These sub-problems concern system layout design and motion planning for single and multi-robot systems, while collision detection is addressed. The sub-problems are handled through ad-hoc developed Mixed Integer Programming (MIP) models. The proposed solution overcomes the limitations of the current design and motion plan approaches. In fact, the design of body-in-white assembly cell and the robot motion planning are two time-expensive and interconnected activities, up to now generally managed from different human operators. The resolution of these two activities as non-interrelated could lead to an increase of the engineer-to-order time and a reduction of the solution quality. Thus, a test bed is described in order to prove the applicability of the approach.

I. INTRODUCTION

Body-in-white assembly consists in the joining of the metal sheets through welding processes [1]. The metal sheets are blocked by a fixturing system and handled by a transporter (Figure 1). The design of these multi-robot cells, *i.e.* the selection of the resources and their placement, and the motion planning of the robots are two critical, human-based and interconnected activities. However, commercial software tools or scientific frameworks able to automatically and simultaneously solve both the problems cannot be found due to the integration complexity. Thus, this paper aims at providing an uniform multi-disciplinary approach and software tool for the optimization of multi-robot spot-welding cell design while identifying feasible robot motion plans.

The design of spot-welding cells has been discussed in the literature mainly focusing on specific aspects of the problem, such as the selection of the welding guns and the position of the robots in the cell, and not considering the influence of the motion plan on the design [1], [2], [3], [4], [5]. An example is presented in [6], where the allocation of the welding points to the robots and the robot trajectories are predefined inputs. An interesting methodology is presented in [7], [8], where, however, collision detection only considers the robot tool center point disregarding the whole robot support structure.

The generation of a collision-free robot trajectory in order to move the robot from its initial configuration to its goal configuration, avoiding static or dynamic obstacles in the environment, is introduced in [9] in relation to generic

robot planning. [10] focuses on off-line motion planning for a single robot that can be solved through different techniques, such as probabilistic potential fields, probabilistic roadmaps, probabilistic cell decomposition and simple-query sampling-based method. Among these techniques, the probabilistic roadmaps have been studied in case of complex environment with anthropomorphic robots [11]. Centralized and decoupled off-line motion planning approaches for interacting robots in generic application are formalized in [12], underlining the advantages and disadvantages of the two approaches. Independently from the selected motion planning technique, collision detection approaches such as swept volume, feature tracking and hierarchical decomposition have to be adopted in order to obtain collision-free trajectories. Swept-volume methods [13] aim at calculating the volume swept by the objects and checking for collision, but are generally characterized by the high cost of their practical implementation. Feature-tracking methods [14] determine if pairs of features are disjoint, thus limiting their applicability to simplified objects characterized by few convex components. Finally, hierarchical decomposition methods [15], [16] pre-compute a hierarchy of bounding volumes (*e.g.* spheres, axis-aligned bounding boxes, oriented bounding boxes) for each object (robot link, obstacle) allowing multi-resolution simulation. Actually, in the authors knowledge, the simultaneous design and motion planning of body-in-white assembly cells has not yet been investigated, and, in addition, the different sub-problems that must be faced to attain the optimum cell design have not been completely solved.

Trying to formalize the problem, the method here presented assumes that the design of spot-welding multi-robot cells can be considered optimal when the selection of the resources and their placement in the cell minimize an objec-

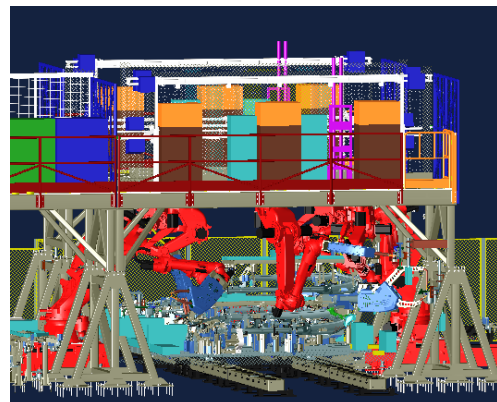


Fig. 1: Multi-robot cells for spot welding - COMAU.

¹ Institute of Industrial Technologies and Automation, National Research Council, via Bassini 15, 20133 Milan, Italy.

² Faculty of Mechanical Engineering, Technion, Haifa 32000, Israel.

³ Faculty of Mechanical Engineering, Politecnico di Milano, Italy.

stefania.pellegrinelli@itia.cnr.it

tive function based on the cost of the acquired resources. At the same time, the welding points are allocated to the robots providing free-collision motion plans for each robot, thus ensuring cell cycle time constraint. The method, depicted in Figure 2, is an iterative algorithm composed by three main consequential sub-problems: (i) identification of all the feasible single-robot motion planning for all the cell designs that satisfy the user constraints, (ii) identification of the multi-robot cell design that minimizes the investment costs and gives a first allocation for the welding points to each robot, (iii) identification of the multi robot coordination that guarantees the respect of the application constraints (*i.e.* the cycle time).

The paper is structured as follows: Section II depicts the problem and the approach; Section III presents a test case for the provided methodology; in Section IV, conclusions and future work are given. A detailed appendix reports the constraint equations used in the model.

II. PROBLEM POSITION AND PROPOSED METHODOLOGY

The aim of the develop approach and the related software tool is to provide an automatic methodology for the generation of an optimized design of a spot-welding multi-cell and a feasible motion plan. As in the industrial practice, the approach requires inputs generally defined by the client:

Client Input.1: the car-body metal sheets, CB ;

Client Input.2: the welding points, WPs ;

Client Input.3: the car body fixture, BF ;

Client Input.4: the cell cycle time, RCT .

Together with the client's inputs, the following inputs have to be selected among all the set of resources available on the market (for nomenclature refer to Table II):

Resources.1: the Robot Model, RM . The method considers one robot model for sake of simplicity and due to the current industrial practice;

Resources.2: the Robot support Structure Model, RSM (same consideration of RM);

Resources.3: the Welding Gun Models, $WGM(s)$. Each robot can be provided by a different WGM ;

Resources.4: the Number of already aCquired Resources, NC^{RM} , NC^{RSM} , $NC^{WGM_{wgm}}$;

Resources.5: Cost of resources, $COST^{RM}$, $COST^{WGM_{wgm}}$, $COST^{RSM}$

Resources.6: Availability of resources α^{RM} , $\alpha^{WGM_{wgm}}$.

The provided solution consists in a set of variables (for nomenclature refer to Table II):

Variables.1: the Total Robot Number, TN^{RM} ;

Variables.2: the Total Number of Welding Gun Models, $TN^{WGM_{wgm}}$;

Variables.3: the Position and Orientation of the Robots in the cell, RPO ;

Variables.4: the allocation of the welding gun models, $RGP_{wgm, rpo}$;

Variables.5: the Welding Points, $WPA_{rpo, wp}^{II}$;

Variables.6: the motion plan for each robot, RMP , $C_{rpo, wp1, wp2}$, $I_{rpo, wp1, wp2}$.

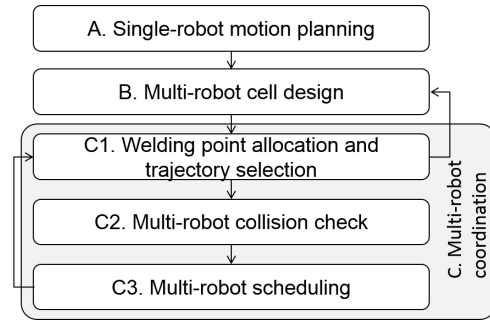


Fig. 2: Framework.

The approach is based on three different steps (Figure 2):

Step A: The first step (single-robot motion planning) aims at identifying all the collision-free trajectories among reachable welding points for the selected robot model and for each position and orientation of the robot in the cell and for each welding gun model.

Step B: The second step concerns the design of the cell layout on the basis of the results of *Step A*. During this step, the welding points are finally allocated to the robots as a first attempt.

Step C: The goal of the third step is the coordination of the robots, *i.e.* each welding point is allocated to one robot (*Step C1*), the motion plan is identified (*Step C1*) and the robot trajectory starting time is defined (*Step C3*) in order to avoid collision among the robots (*Step C2*). The steps are hereafter described.

A dedicated sub-section for each Step is hereafter reported.

A. Single-Robot Motion Planning

The first step aims at defining possible motion plans considering one robot position and orientation (RPO_{rpo}) and one welding gun model (WGM_{wgm}) at a time. Thus, the idea is to define all the possible combination $\langle RPO_{rpo}, WGM_{wgm} \rangle$ and for each combination to identify: (i) the reachable welding points; (ii) robot collision-free trajectories among the reachable welding points. In order to automatically define the trajectories, probabilistic roadmap are exploited together with the Open Robot Library - ORL - (robot motion planner module of COMAU controllers [17]) for trajectory definition and the RAPID library [15] for fast collision detection. The generation of the roadmap is structured in six steps:

Step A1 defines through the ORL which welding points can be reachable from the robot, *i.e.* which welding points belong to the robot workspace and do not cause robot singularities.

Step A2 concerns the sampling of the joint space. The sampled points are added to the sampled space if they do not lead to a robot singularity and are collision free. Three main techniques have been tested in order to sample the joint space [18]: the *Grid* method¹, *Random* algorithm², and the

¹The motion range of each joint is divided according to a fixed value n that changes according to the motion range of the joints. The joint characterized by a wider motion range presents a high value of n . However, even for small n , the number of sampled points is elevated.

²The sample space is created choosing random values for each robot joint.

Halton method³. The *Halton* method has been chosen since it grants a better trade-off between computational time and uniform sampling.

Step A3 Sampled points are connected in order to obtain a roadmap. Specifically, points can be connected according to different techniques. Up to now, the *nearest-n* technique has been employed: each sampled point is connected to the nearest n points. The distance between two configurations can be evaluated on the basis of two different criteria. Since the goal of the approach is the reduce the cell cycle time, the first criterion is the trajectory time provided by the ORL. The second criteria is the area swept by the robot [11] for reaching the second configuration being in the first configuration. The trajectories provided by the ORL are checked for collisions by the RAPID library. According to [18], a *binary* collision check method has been implemented. This algorithm starts from the middle point and if it is collision free, both the halves of the path are checked in the middle position. The algorithm stops when the distance between two adjacent positions is less than ϵ .

Step A4 consists in the connection of the pairs of reachable welding points to the generated roadmap. First, the point of the roadmap nearer to the welding point is selected. If a collision-free path between the selected point and the welding point can be found by the ORL the points are connected. Otherwise, the second point nearer to the welding point will be selected and tested for collision-free path. The algorithm ends when a connection is established.

Step A5 defines the collision-free path to move from the first welding point to the second. Specifically, the shortest path is obtained through the employment of the A* algorithm [19]. *Step A6* allows the generation of the free trajectory between the selected welding points on the basis of the path found in *Step A5*. In order to reduce the motion time, a fly trajectory is defined. The process is iterative: for each middle point of the trajectory, a fly distance is imposed. If during the trajectory a collision is found, the fly distance is reduced.

B. Multi-Robot Cell design

Step B aims at solving the multi-robot cell design problem resulting in the enumeration of the robot positions/orientations and the selection of a welding gun model for each robot. In order to cope with the cell cycle time, a first-attempt motion plan is provided. This motion plan stands on the hypothesis that the welding points can be associated to more than one robot, so that the computational effort for the model resolution is reduced and the remaining degrees of freedom can be exploited during robot coordination. Indeed, in *Step C* the allocation of the welding points to each robot will be revised and the one-to-one allocation (each welding point to one robot) will be satisfied.

The proposed model, partially addressed in [20], is an innovative formalization of the problem successively described as a MIP (Mixed Integer Programming) in terms of parameters, variables, objective functions and constraints.

³Halton points are used in order to reach a better coverage of the region.

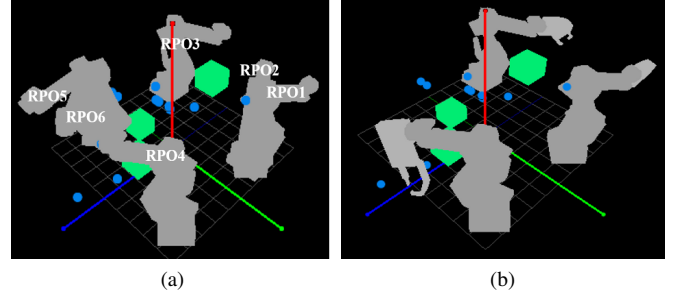


Fig. 3: Simulation of the Cell. (a) Test bed environment: for two robots only one RPO is admissible, while for two robots two $RPOs$ are possible. (b) Attained cell design.

The algorithm spans the whole set of solutions elaborated in *Step A*, identifying a sub-set of them such that the total investment cost is minimized. The selected objective function is specified in (1) and takes into account the cost of the acquired resources that is equal to the number of resources required by the system minus the number of already acquired resources; a penalty cost PC whenever exceeding the cycle time; a term introduced to minimize the intersection between the robot working areas given the robot positions and orientations SIA_{rpo_1, rpo_2} . The influence on the objective function of this last term not related to cost issue is reduced by its multiplication with a low constant value L . The model is based on 29 constraints presented in the appendix and related to the resources, motion planning and cycle time.

$$\min \left\{ NA^{RM} \cdot COST^{RM} + \sum_{wgm} (NA^{WGM_{wgm}} \cdot COST^{WGM_{wgm}}) \right. \\ \left. + NA^{RSM} \cdot COST^{RSM} + PC \cdot MCT + L \sum_{rpo_1, rpo_2} SIA_{rpo_1, rpo_2} \right\} \quad (1)$$

C. Multi-Robot Coordination

Step C is divided into three sub-steps whose goal is to define the allocation of the welding points to the robots, while selecting the trajectories that minimize the cycle time; to simultaneously simulate the trajectories of two robots in order to find out possible collisions among the robots; to exploit the information related to the possible robot collisions to redefine the starting time of the trajectories through a scheduling model for robot coordination. The three sub-steps are hereafter described.

C1 - Welding point allocation and trajectory selection. Considering the cell layout in *Step B*, *Step C1* is based on a MIP model that minimizes the cell cycle time and allocates the welding points one-to-one with the robots (2). The meaning of the objective function is given by (C1.14)(C1.15). 15 constraints (see Appendix), grant the correctness of the motion plan (motion plan constraints) and the respect of the maximum cycle time (cycle time constraints).

$$\min \{ MAXOCT \} \quad (2)$$

C2 - Multi-robot collision check. *Step C1* provides a motion plan that grants the absence of collisions among the robots and the obstacles. However, collisions among robots may

occur. Thus, the aim of *Step C2* is to check the motion plan defined by *Step C1* for collisions among robots, considering all the possible couples of trajectories.

C3 - Multi-robot scheduling. On the basis of the analysis provided by *Step C2*, *Step C3* schedules the execution of the welding points so that robots resulting in possible collisions cannot be in the same place at the same time. Thus, if necessary, it shifts the starting time I_{rpo,wp_1,wp_2} and the completion time C_{rpo,wp_1,wp_2} for each single-robot motion plan. The step is based on a MIP model that modifies the motion plan provided by *Step C2* in order to minimize the cell cycle time, while coordinating the robots. The objective function is presented in (3). Apart from the obtained cell cycle time $MAXOCT$, the function allows the minimization of three variables: the cycle time of each robots OCT_{rpo} , the trajectory starting I_{rpo,wp_1,wp_2} and completion C_{rpo,wp_1,wp_2} time. These variables are multiplied for a reduction coefficient L not to influence the minimization of $MAXOCT$, which is the main goal of the model. The 10 constraints are presented in the appendix. The proposed model differs from existing models [21], since it copes with articulated robots independently from the shape of the links.

$$\min \left\{ MAXOCT + L \left\{ \sum_{rpo,wp_1,wp_2} (I_{rpo,wp_1,wp_2} + C_{rpo,wp_1,wp_2}) + \sum_{rmp_1,rmp_2} (SF_{rmp_1,rmp_2} + SS_{rmp_1,rmp_2}) + \sum_{rpo} OCT_{rpo} \right\} \right\} \quad (3)$$

III. APPLICATION AND RESULTS

The feasibility of the described approach is shown on an ad-hoc test case hereafter described. A ground structure with 6 possible positions/orientations for the robot and 3 obstacles are considered (Figure 3a) for the welding of 13 WP_s . The model of the robot is the SMART-5 NJ4-175-2.2 on which 2 different welding gun models can be mounted. The inputs are resumed in Table I. *Step A* consists in the definition of 16 roadmaps ($RPO \cdot WGM = 16$) built in order to identify the collision-free trajectories for each possible "robot position/orientation and welding gun model". The roadmap generated for RPO_1 and WGM_1 is represented in Figure 4a together with the trajectory connecting the initial position of the robot in RPO_1 and the WP_6 (Figure 4b). 150 points are sampled according to the Halton techniques from the robot joint space and each sampled point is connected to the 15 nearest points, where nearest implies a time connotation. The collision-detection frequency is 10 Hz. *Step B* leads to the definition of the cell design as depicted in Figure 3b: robots in RPO_1 , RPO_3 and RPO_4 are selected; they respectively mount WGM_2 , WGM_2 and WGM_1 and are responsible for the welding of 7, 3 and 8 WP_s with a cycle time equal to $OCT_1 = 120s$, $OCT_2 = 36s$ and $OCT_4 = 65s$. The total cost of the cell is 336.000 €. The final motion plan is generated through *Step C* leading to the results presented in Table I. The robot cycle time decreases for the robot in RPO_1 and RPO_2 , since the WP_s are univocally allocated to the robots. On the contrary, the robot cycle time of the robot in RPO_4

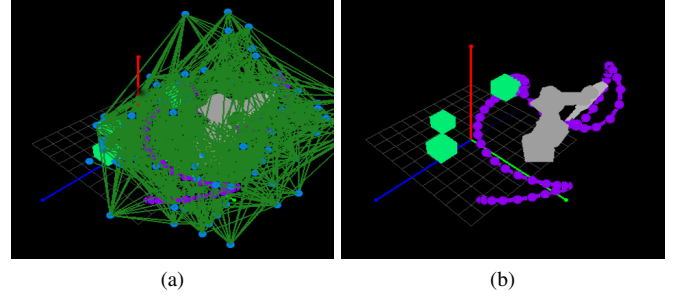


Fig. 4: Robot Trajectories: (a) Roadmap of RPO_1 and WGM_1 . (b) Trajectory connecting the initial position of the robot in RPO_1 and the WP_6 .

increases because of the coordination action that shifts the execution time of the trajectories.

The approach has been implemented in C++ in an ad-hoc software tool partially integrating some existent open-source/commercial libraries. The resolution of the here described problem required 8 hours on a 2.66GHz processor laptop for *Step A* and few seconds for *Step B* and *Step C*.

IV. CONCLUSION AND FUTURE WORK

The proposed approach provides a new automated methodology for the simultaneous design of spot-welding cells and the definition of the robot motion plan. The approach results to be innovative since it takes into account the influence of the motion plan on the cell design, providing single-robot collision-free trajectories as inputs to the cell design. From the industrial point of view, the developed software tool could support human operator activities through the generation of a set of alternative solutions, differing in the robot support structure or in the robot model. Future work will concerns the integration of the methodology with modules for the evaluation of the robot energy consumption, thus moving towards sustainability in manufacturing and life cycle costs.

REFERENCES

- [1] A. Al-Zaher and W. ElMaraghy, "Design of reconfigurable automotive framing system," *CIRP Annals - Manuf. Tech.*, vol. 62, pp. 491–494, 2013.
- [2] P. Bhangale, V. Agrawal, and S. Saha, "Attribute based specification, comparison and selection of a robot," *Mechanism and Machine Theory*, vol. 39, pp. 1345–1366, 2004.
- [3] M. Sarkans and L. Roosimolder, "Welding robot cell implementation in sme-s using modular approach - case study," in *7th Int. DAAAM Baltic Conf. 'INDUSTRIAL ENGINEERING'*, 2010.
- [4] R. V. Rao, B. K. Patel, and M. Parnichkun, "Industrial robot selection using a novel decision making method considering objective and subjective preferences," *Rob. and Aut. Sys.*, vol. 59, pp. 367–375, 2011.
- [5] R. Kumar and R. K. Garg, "Optimal selection of robots by using distance based approach method," *Rob. and CIM*, vol. 26, no. 5, pp. 500–506, 2010.
- [6] G. Michalos, S. Makris, and D. Mourtzis, "An intelligent search algorithm-based method to derive assembly line design alternatives," *Int. J. of Comp. Int. Man.*, vol. 25, no. 3, pp. 211–229, 2012.
- [7] N. Papakostas and *et al.*, "Industrial applications with cooperating robots for the flexible assembly," *Int. J. of Comp. Int. Man.*, vol. 24, no. 7, pp. 650–660, 2011.

TABLE I: Synthesis of the COMAU case.

$N^{WP} : 3$, $BF : 3$ parallelepipeds, $RCT : 120$ $WT_k : 3, \forall k = 1, \dots, 13$														
Client Inputs	WP_1	WP_2	WP_3	WP_4	WP_5	WP_6	WP_7	WP_8	WP_9	WP_{10}	WP_{11}	WP_{12}	WP_{13}	
	1500.57	441.63	-659.36	601.99	97.33	-689.36	2698.07	-1592.62	1201.99	601.99	-689.36	-689.36	-689.36	
	-181.52	-1449.19	-784.45	-1298.56	1802.31	-784.45	327.73	-767.12	-1098.56	-1098.56	-1284.45	-1284.45	-1184.45	
	31.02	-770.59	357.20	1165.64	2403.67	257.20	966.75	-191.64	195.64	1165.64	257.20	657.20	257.20	
	-58.26	+134.71	-156.36	-139.71	68.70	-166.36	-87.68	149.63	-59.71	-139.71	-166.36	-166.36	-166.36	
	148.37	+164.12	92.54	108.49	35.56	92.54	96.95	163.70	108.49	108.49	92.54	92.54	92.54	
	-126.83	+131.02	77.26	-80.62	70.39	77.26	159.24	149.38	-60.62	-80.62	77.26	77.26	77.26	
Resources	$RM : 1$ (COMAU SMART-5-NJ4-175-2.2).													
	$RSM : 1$ (Ground support structure).													
	$N^{RPO} : 6$ (4 possible positions with respectively 2, 1, 2 and 1 possible orientations).													
	$N^{WGM} : 2,$		$WGM_1 : vcgca131001$			$WGM_2 : vcgsg001001.$								
	$NC^{RM} : 0,$		$NC^{WGM_1} : 0,$			$NC^{WGM_2} : 0,$		$NC^{RS} : 0.$						
	$COST^{RM} : 1e5,$		$COST^{WGM_1} : 1e3,$			$COST^{WGM_2} : 800.$								
	$\alpha^{WGM_1} : 0.98$		$\alpha^{WGM_2} : 0.95,$			$\alpha^{RM} : 0.95.$								
Program Con- straints	$PC : 10000000$													
	$WP^{COV} : 2$													
	$IGP_{rpo1, rpo2} : [01000000; 10000000; 00100000; 00100000; 00000000; 00000011; 00000101; 00000110]$													
Results														
	RPO_1			RPO_2			RPO_4							
	$N^{WP} : 5$			1			7							
	$wp_1, \dots, wp_s : 9 \rightarrow 3 \rightarrow 12 \rightarrow 6 \rightarrow 7$			2			$8 \rightarrow 1 \rightarrow 4 \rightarrow 5 \rightarrow 10 \rightarrow 13 \rightarrow 11$							
$OCT_{rpo} : 112$			17			78								

- [8] N. Papakostas, K. Alexopoulos, and A. Kopanakis, "Integrating digital manufacturing and simulation tools in the assembly design process: A cooperating robots cell case," *CIRP J. of Man. Sci. and Tech.*, vol. 4, pp. 96–100, 2011.
- [9] J. Latombe, "Robot motion planning," 1991.
- [10] S. LaValle, "Planning algorithms," p. 842, 2006.
- [11] L. Kavraki, P. Svestka, J.-C. Latombe, and M. Overmars, "Probabilistic roadmaps for path planning in high-dimensional configuration spaces," *IEEE Tran. on Aut. Con., Rob. and Aut.*, vol. 12, pp. 566 – 580, 1996.
- [12] G. Sanchez and J. Latombe, "Using rpm planner to compare centralized and decoupled planning for multi-robot systems," in *Proc. IEEE Int. Conf. on Rob. and Aut.*, 2002.
- [13] H. Taubig, B. Bauml, and U. Frese, "Real-time swept volume and distance computation for self collision detection," in *IEEE/RSJ Int. Conf. on Int. Rob. and Sys. (IROS)*, 2011.
- [14] S. H. Lee, K. Y. Lee, Y. Woo, and K. S. Lee, "Feature-based multi-resolution modeling of solids using history-based boolean operations - part ii: Implementation using a non-manifold modeling system," *J. of Mech. Sci. and Tech.*, vol. 19, no. 2, pp. 558–566, 2005.
- [15] S. Gottschalk, M. C. Lin, and D. Manocha, "Obbtrees: A hierarchical structure for rapid interference detection," *SIGGRAPH Proc. of the 23rd Conf. on Comp. Graph. and Inter. Tech.*, pp. 171–180, 1996.
- [16] S. Azernikov, A. Miropolsky, and A. Fischer, "Surface reconstruction of freeform objects based on multiresolution volumetric method," in *Proc. of the eighth ACM symposium on Solid modeling and applications*, 2003, pp. 115–126.
- [17] <http://www.comau.com>, 2013.
- [18] R. Geraerts and M. Overmars, *A Comparative Study of Probabilistic Roadmap Planners*. Springer, 2004, vol. 7, pp. 43–58.
- [19] R. Dechter and J. Pearl, "Generalized best-first search strategies and the optimality of a*," *J. of the ACM*, vol. 32, no. 3, 1985.
- [20] S. Pellegrinelli, N. Pedrocchi, L. M. Tosatti, and T. Tolio, "Integrated approach for multi-robot spot-welding cell design and welding-point allocation," *Key Engineering Materials*, vol. 572, pp. 648–651, 2014.
- [21] J. Peng and S. Akella, "Coordinating multiple robots with kinodynamic constraints along specified paths," *Int. J. of Robotics Research*, vol. 24, no. 4, pp. 295–310, 2005.

APPENDIX

A. Main constraints for Step B model

Resources Constraints

$$TN^{RM'} = TN^{RM} - NC^{RM} \quad (B.1)$$

$$NA^{RM} \geq TN^{RM'} \quad (B.2)$$

$$TN^{WGM'}_{wgm} = TN^{WGM}_{wgm} - NC^{WGM}_{wgm} \quad (B.3)$$

$$NA^{WGM}_{wgm} \geq TN^{WGM'}_{wgm} \quad \forall wgm \quad (B.4)$$

$$NA^{RSM} = 1 - NC^{RSM} \quad (B.5)$$

$$\sum_{wgm} TN^{WGM}_{wgm} = TN^{RM} \quad (B.6)$$

$$\sum_{rpo} RGP_{wgm, rpo} = TN^{RM} \quad (B.7)$$

$$\sum_{rpo} RGP_{wgm, rpo} = TN^{WGM}_{wgm} \quad \forall wgm \quad (B.8)$$

$$\sum_{wgm} (RGP_{wgm, rpo1} + RGP_{wgm, rpo2}) IGP_{rpo1, rpo2} \leq 1 \quad (B.9)$$

$$\sum_{rpo1, rpo2} BIA_{rpo1, rpo2} \geq \sum_{wgm} (RGP_{wgm, rpo1} + RGP_{wgm, rpo2}) - 1 \quad \forall rpo1, rpo2 \quad (B.10)$$

$$\sum_{rpo1, rpo2} BIA_{rpo1, rpo2} \geq \frac{1}{2} \sum_{wgm} (RGP_{wgm, rpo1} + RGP_{wgm, rpo2}) \quad \forall rpo1, rpo2 \quad (B.11)$$

$$SIA_{rpo1, rpo2} = I A_{rpo1, rpo2} BIA_{rpo1, rpo2} \quad \forall rpo1, rpo2 \quad (B.12)$$

Motion planning constraints

$$\sum_{wp} WPA_{rpo,wp}^I \leq L^{-1} \sum_{wgm} RGP_{wgm,rpo} \quad \forall rpo \quad (B.13)$$

$$\sum_{wp} WPA_{rpo,wp}^I \geq \sum_{wgm} RGP_{wgm,rpo} \quad \forall rpo \quad (B.14)$$

$$\sum_{rpo} WPA_{rpo,wp}^I \leq WP^{COV} \quad \forall wp \neq 0 \quad (B.15)$$

$$\sum_{rpo} WPA_{rpo,0}^I = TN^{RM} \quad (B.16)$$

$$\sum_{rpo} WPA_{rpo,wp}^I \geq 1 \quad \forall wp \quad (B.17)$$

$$\sum_{wgm,wp_2} MP_{wp,wp_2}^{wgm,rpo} = WPA_{rpo,wp}^I \quad \forall rpo,wp \quad (B.18)$$

$$\sum_{wgm,wp_1} MP_{wp_1,wp}^{wgm,rpo} = WPA_{rpo,wp}^I \quad \forall rpo,wp \quad (B.19)$$

$$MP_{wp_1,wp_2}^{wgm,rpo} \leq MP_{wp_1,wp_2}^{f,wgm,rpo} \quad \forall wgm,rpo,wp_1,wp_2 \quad (B.20)$$

$$\sum_{wp_1,wp_2} MP_{wp_1,wp_2}^{wgm,rpo} \leq L^{-1} RGP_{wgm,rpo} \quad \forall wgm,rpo \quad (B.21)$$

$$\sum_{wp_1,wp_2} MP_{wp_1,wp_2}^{wgm,rpo} \geq RGP_{wgm,rpo} \quad \forall wgm,rpo \quad (B.22)$$

$$\sum_{wp} MPS_{wgm,rpo,0,wp} = RGP_{wgm,rpo} \quad \forall wgm,rpo \quad (B.23)$$

$$\sum_{wgm,wp_2} MPS_{wp,wp_2}^{wgm,rpo} - \sum_{wgm,wp_1} MPS_{wp_1,wp}^{wgm,rpo} = WPA_{rpo,wp}^I \quad \forall rpo,wp \neq 0 \quad (B.24)$$

$$MP_{wp_1,wp_2}^{wgm,rpo} \geq MPS_{wp_1,wp_2}^{wgm,rpo} \setminus WP \quad \forall wgm,rpo,wp_1,wp_2 \quad (B.25)$$

Cycle time constraints

$$OCT_{rpo} = \frac{\sum_{wgm,wp_1,wp_2} MT_{wp_1,wp_2}^{wgm,rpo} MP_{wp_1,wp_2}^{wgm,rpo}}{\alpha^{RM}} \quad (B.26)$$

$$+ \sum_{wgm,wp_1,wp_2} \frac{MP_{wp_1,wp_2}^{wgm,rpo} WT_{wp_1}}{\alpha^{WGM_{wgm}}} \quad \forall rpo$$

$$OCT_{rpo} \leq MAXOCT \quad \forall rpo \quad (B.27)$$

$$SCT = MAXOCT - RCT \quad (B.28)$$

$$MCT \geq SCT \quad (B.29)$$

B. Main constraints for Step C1 model

Motion planning constraints

$$\sum_{wp} WPA_{rpo,wp}^{II} \leq L^{-1} \sum_{wgm} RGP_{wgm,rpo} \quad \forall rpo \quad (C1.1)$$

$$\sum_{wp} WPA_{rpo,wp}^{II} \geq \sum_{wgm} RGP_{wgm,rpo} \quad \forall rpo \quad (C1.2)$$

$$\sum_{rpo} WPA_{rpo,wp}^{II} = 1 \quad \forall wp \neq 0 \quad (C1.3)$$

$$WPA_{rpo,wp}^{II} \leq WPA_{rpo,wp}^I \quad \forall rpo,wp \quad (C1.4)$$

$$\sum_{rpo} WPA_{rpo,0}^{II} = TN^{RM} \quad (C1.5)$$

$$\sum_{wgm,wp_2} MP_{wp,wp_2}^{wgm,rpo} = WPA_{rpo,wp}^{II} \quad \forall rpo,wp \quad (C1.6)$$

$$\sum_{wgm,wp_1} MP_{wp_1,wp}^{wgm,rpo} = WPA_{rpo,wp}^{II} \quad \forall rpo,wp \quad (C1.7)$$

$$MP_{wp_1,wp_2}^{wgm,rpo} \leq MP_{wp_1,wp_2}^{f,wgm,rpo} \quad \forall wgm,rpo,wp_1,wp_2 \quad (C1.8)$$

$$\sum_{wp_1,wp_2} MP_{wp_1,wp_2}^{wgm,rpo} \leq L^{-1} RGP_{wgm,rpo} \quad \forall wgm,rpo \quad (C1.9)$$

$$\sum_{wp_1,wp_2} MP_{wp_1,wp_2}^{wgm,rpo} \geq RGP_{wgm,rpo} \quad \forall wgm,rpo \quad (C1.10)$$

$$\sum_{wp} MPS_{wgm,rpo,0,wp} = RGP_{wgm,rpo} \quad \forall wgm,rpo \quad (C1.11)$$

$$WPA_{rpo,wp}^{II} = \sum_{wgm,wp_2} MPS_{wp_1,wp_2}^{wgm,rpo} - \sum_{wgm,wp_1} MPS_{wp_1,wp_2}^{wgm,rpo} \quad \forall rpo,wp \neq 0 \quad (C1.12)$$

$$MP_{wp_1,wp_2}^{wgm,rpo} \geq MPS_{wp_1,wp_2}^{wgm,rpo} \setminus WP \quad \forall wgm,rpo,wp_1,wp_2 \quad (C1.13)$$

Cycle time constraints

$$OCT_{rpo} = \frac{\sum_{wgm,wp_1,wp_2} MT_{wp_1,wp_2}^{wgm,rpo} MP_{wp_1,wp_2}^{wgm,rpo}}{\alpha^{RM}} \quad (C1.14)$$

$$+ \sum_{wgm,wp_1,wp_2} \frac{MP_{wp_1,wp_2}^{wgm,rpo} WT_{wp_1}}{\alpha^{WGM_{wgm}}} \quad \forall rpo$$

$$OCT_{rpo} \leq MAXOCT \quad \forall rpo \quad (C1.15)$$

C. Main constraints for Step C3 model

Motion planning constraints

$$MTT_{rpo,wp_1,wp_2} = \frac{\sum_{wgm} MP_{wp_1,wp_2}^{wgm,rpo} MT_{wp_1,wp_2}^{wgm,rpo}}{\alpha^{RM}} \quad (C3.1)$$

$$+ \sum_{wgm} \frac{WPA_{rpo,wp_2}^{II} WT_{wp_2} MP_{wp_1,wp_2}^{wgm,rpo}}{\alpha^{WGM_{wgm}}} \quad \forall rpo,wp_1,wp_2$$

$$I_{rpo^{rpm},wp_1^{rpm},wp_2^{rpm}} \geq 0 \quad \forall rpm \mid wp_1^{rpm} = 0 \quad (C3.2)$$

$$I_{rpo^{rpm},wp_1^{rpm},wp_2^{rpm}} \geq I_{rpo^{rpm-1},wp_1^{rpm-1},wp_2^{rpm-1}} + MTT_{rpo^{rpm-1},wp_1^{rpm-1},wp_2^{rpm-1}} \quad \forall rpm \mid wp_1^{rpm} \neq 0 \quad (C3.3)$$

$$C_{rpo^{rpm},wp_1^{rpm},wp_2^{rpm}} = I_{rpo^{rpm+1},wp_1^{rpm+1},wp_2^{rpm+1}} \quad \forall rpm \mid wp_2^{rpm} \neq 0 \quad (C3.4)$$

$$C_{rpo^{rpm},wp_1^{rpm},wp_2^{rpm}} \geq I_{rpo^{rpm},wp_1^{rpm},wp_2^{rpm}} + MTT_{rpo^{rpm},wp_1^{rpm},wp_2^{rpm}} \quad \forall rpm \mid wp_2^{rpm} = 0 \quad (C3.5)$$

$$L \cdot SF_{rpm_1,rpm_2} BB_{rpm_1,rpm_2} \geq \left(C_{rpo^{rpm_1},wp_1^{rpm_1},wp_2^{rpm_1}} - I_{rpo^{rpm_2},wp_1^{rpm_2},wp_2^{rpm_2}} \right) BB_{rpm_1,rpm_2} \quad \forall rpm_1,rpm_2 \quad (C3.6)$$

$$L \cdot SS_{rpm_1,rpm_2} BB_{rpm_1,rpm_2} \geq \left(C_{rpo^{rpm_2},wp_1^{rpm_2},wp_2^{rpm_2}} - I_{rpo^{rpm_1},wp_1^{rpm_1},wp_2^{rpm_1}} \right) BB_{rpm_1,rpm_2} \quad \forall rpm_1,rpm_2 \quad (C3.7)$$

$$(SF_{rpm_1,rpm_2} + SS_{rpm_1,rpm_2}) BB_{rpm_1,rpm_2} \leq 1 \quad \forall rpm_1,rpm_2 \quad (C3.8)$$

Cycle time constraints

$$OCT_{rpo} \geq C_{rpo,wp_1,wp_2} \quad \forall rpo,wp_1,wp_2 \quad (C3.9)$$

$$OCT_{rpo} \leq MAXOCT \quad \forall rpo \quad (C3.10)$$

TABLE II: Parameters and variable definitions. I and O indicate that is an Input or an Output of the corresponding Step.

Symbol	Inputs/Outputs Description	A	B	C1	C2	C3
CB	Car body	I	I	I	I	I
BF	Car-Body Fixture	I	I	I	I	I
$WP_{wp}, wp \in \{1, \dots, N^{WP}\}$	Welding Point(s) expressed as position [mm] and rotation [$^{\circ}$] respect to cell reference system. N^{WP} denotes the number of WPs	I	I	I	I	I
RM	Robot Model. The RM is imposed to be the same for all the robots	I	-	-	I	-
RSM	Robot support Structure Model.	I	-	-	I	-
$RPO_{rpo}, rpo \in \{1, \dots, N^{RPO}\}$	Robot Position/Orientation. N^{RPO} denotes the number of possible $RPO(s)$	I	I	I	I	I
$WGM_{wgm}, wgm \in \{1, \dots, N^{WGM}\}$	Welding Gun Model(s). N^{WGM} denotes the number of possible $WGM(s)$	I	I	I	I	I
$RMP_{rmp}, rmp \in \{1, \dots, N^{RMP}\}$	Each Robot Motion Plan corresponds to a possible terms of indexes $\{rpo, wp_1, wp_2\}$. N^{RMP} indicates all the possible combinations (feasible Robot Motion Plan)					
$rpo^{rpm} = RMP_{rmp}.rpo \in \mathbb{N}$	rpo^{rpm} is the index of RPO_{rpo} extracted from RMP_{rmp}					
$wp_1^{rpm} = RMP_{rmp}.wp_1 \in \mathbb{N}$	wp_1^{rpm} is the index of WP_{wp_1} extracted from RMP_{rmp}					
$wp_2^{rpm} = RMP_{rmp}.wp_2 \in \mathbb{N}$	wp_2^{rpm} is the index of WP_{wp_2} extracted from RMP_{rmp}					
$NC^{RM} \in \mathbb{N}$	Number of already aCquired Robot for each RM	I	-	-	-	-
$NC^{WGM_{wgm}} \in \mathbb{N}$	Number of already aCquired Welding Gun Models for each WGM_{wgm}	I	-	-	-	-
$NC^{RSM} \in \{0,1\}$	Number of already aCquired Robot Structures	I	-	-	-	-
$\alpha^{WGM_{wgm}}$	WGM availability [%]	-	I	I	-	I
α^{RM}	RM availability [%]	-	I	I	-	I
$WT_{wp} \in \mathbb{R}^+$	Welding Time for each WP [s]	-	I	I	-	I
$RCT \in \mathbb{R}^+$	Required Cycle Time [s]	-	I	I	-	I
$COST^{RM} \in \mathbb{R}^+$	Cost per unit [€]	-	I	-	-	-
$COST^{WGM_{wgm}} \in \mathbb{R}^+$	Cost per unit of WGM [€]	-	I	-	-	-
$COST^{RSM} \in \mathbb{R}^+$	Cost per unit [€]	-	I	-	-	-
$PC \in \mathbb{R}^+$	Penalty Cost for each lost time unit [€/s]	-	I	-	-	-
$WP^{COV} \in \mathbb{N}$	Maximum Number of robots to which it is possible to associate a WP	-	I	-	-	-
$IGPrpo_1, rpo_2 \in \{0,1\}$	Equal to 0 if the robot in RPO_{rpo_1} and the robot in RPO_{rpo_2} display the same position and a different orientation; otherwise 1	-	I	-	-	-
$IA_{rpo_1, rpo_2} \in \mathbb{R}^+$	Percentage representing the intersection area between the working area of the robot in RPO_{rpo_1} and the working area of the robot in RPO_{rpo_2}	-	I	-	-	-
$NA^{WGM_{wgm}} \in \mathbb{N}$	Number of Welding Guns to be Acquired for each WGM	-	O	-	-	-
$NA^{RSM} \in \{0,1\}$	Number of Robot Structures to be Acquired	-	O	-	-	-
$NA^{RM} \in \mathbb{N}$	Number of Robot to be Acquired	-	O	-	-	-
$SIA_{rpo_1, rpo_2} \in \mathbb{R}^+$	If robot in RPO_{rpo_1} and robot in RPO_{rpo_2} are selected, SIA_{rpo_1, rpo_2} represents the intersection of their working areas	-	O	-	-	-
$BIA_{rpo_1, rpo_2} \in \{0,1\}$	Equal to 1 if robot in RPO_{rpo_1} and robot in RPO_{rpo_2} are selected, otherwise 0	-	O	-	-	-
$TN^{WGM_{wgm}} \in \mathbb{Z}$	Total Number of selected Welding Guns for each WGM	-	O	-	-	-
$TN^{WGM'_{wgm}} \in \mathbb{N}$	Support variable for the definition of $TN^{WGM_{wgm}}$	-	O	-	-	-
$TN^{RM} \in \mathbb{Z}$	Total Number of Robots	-	O	-	-	-
$TN^{RM'} \in \mathbb{N}$	Support variable for the definition of TN^{RM}	-	O	-	-	-
$OCT_{rpo} \in \mathbb{R}^+$	Obtained Cycle Time for robot in RPO_{rpo} [s]	-	O	O	-	O
$MAXOCT \in \mathbb{R}^+$	Obtained Cycle Time for the cell design [s]	-	O	O	-	O
$MCT \in \mathbb{R}^+$	possible Missing Cycle Time cell design [s]	-	O	-	-	-
$MCTS \in \mathbb{R}$	Support variable for the evaluation of the Missing Cycle Time cell design [s]	-	O	-	-	-
$MPf_{wp_1, wp_2}^{wgm, rpo} \in \{0,1\}$	Equal to 1 if robot in RPO can process WP_{wp_2} immediately after the WP_{wp_1} ; 0 otherwise	O	I	I	-	-
$MP_{wp_1, wp_2}^{wgm, rpo} \in \{0,1\}$	Motion Plan for robot in RPO_{rpo} , with WGM_{wgm} from WP_{wp_1} to WP_{wp_2} - equal to 1 if robot in RPO_{rpo} processes WP_{wp_1} immediately after the WP_{wp_1}	-	O	O	I	I
$MT_{wp_1, wp_2}^{wgm, rpo} \in \mathbb{R}^+$	Motion Time according to $MP_{wp_1, wp_2}^{wgm, rpo}$ [s]	O	I	I	I	I
$MPS_{wp_1, wp_2}^{wgm, rpo} \in \mathbb{N}$	Execution sequence of the WPs for each robot - equal to k if robot in RPO processes WP_{wp_2} immediately after the WP_{wp_1} as kth points.	-	O	O	I	-
$RGP_{wgm, rpo} \in \{0,1\}$	Allocation of the welding guns to the robots	-	O	I	I	-
$WPA_{rpo, wp}^I \in \{0,1\}$	First attempt allocation of WP_{wp} to the robot in RPO_{rpo}	-	O	I	-	-
$WPA_{rpo, wp}^{II} \in \{0,1\}$	Final allocation of WP_{wp} to the robot in RPO_{rpo}	-	-	O	I	I
BB_{rmp_1, rmp_2}	Equal to 1 if the robot in RPO_{rpo} while moving from $WP_{wp_1}^{rpm_1}$ to $WP_{wp_2}^{rpm_1}$ intersects the robot in RPO_{rpo} while moving from $WP_{wp_1}^{rpm_2}$ to $WP_{wp_2}^{rpm_2}$	-	-	-	O	I
$MTT_{rpo, wp_1, wp_2} \in \mathbb{R}$	Time necessary for robot in RPO_{rpo} to move from WP_{wp_1} to WP_{wp_2} and weld WP_{wp_2}	-	-	-	-	O
$Crpo, wp_1, wp_2 \in \mathbb{R}^+$	Competition time for robot in RPO_{rpo} to move from WP_{wp_1} to WP_{wp_2} and weld WP_{wp_2}	-	-	-	-	O
$I_{rpo, wp_1, wp_2} \in \mathbb{R}^+$	Starting time for robot in RPO_{rpo} to move from WP_{wp_1} to WP_{wp_2} and weld WP_{wp_2}	-	-	-	-	O
$SF_{rmp_1, rmp_2} \in \{0,1\}$	Support variable for the definition of BB_{rmp_1, rmp_2}	-	-	-	-	O
$SS_{rmp_1, rmp_2} \in \{0,1\}$	Support variable for the definition of BB_{rmp_1, rmp_2}	-	-	-	-	O
L	low value constant	-	I	I	-	I